Transactions on Additive Manufacturing Meets Medicine
Trans. AMMM, Vol. 4, No 1, Article ID 670, 4 Pages

Original Research Article

3D printed silicone spinal cord implant with sub-millimeter feature size

L. Rennpferdt[1*], P. Kleinschnittger[2], A. Bahr[2,3], and H. K. Trieu[1]

[1] *Institute of Microsystems Technology, Hamburg University of Technology, Hamburg, Germany*
[2] *Institute for Integrated Circuits, Hamburg University of Technology, Hamburg, Germany*
[3] *Sensor System Electronics, Institute of Electrical Engineering and Information Technology, Kiel University, Kiel, Germany*
[*] *Corresponding author, email: lukas.rennpferdt@tuhh.de*

Abstract: Spinal cord injury (SCI) can lead to the dysfunction of nerve fibers by hemi- or complete transection, resulting in permanent paraplegia. In recent years, a number of therapies have been developed to treat spinal cord injury. A mechanical microconnector system (mMS) that supports the regeneration of nerve fibers after SCI through a combination of different therapies was designed in previous works. For this implantable mMS with minimum feature size of a few hundreds of micrometers, it is essential to provide fast, flexible, three-dimensional fabrication. This paper describes a new fabrication method of the mMS made of silicone using additive manufacturing based on a commercially available material jetting printer. The application of this technology advances the fabrication and adaptability of mMS in terms of higher elasticity of the implant using silicone and additionally with respect to high customizability and rapid prototyping using additive manufacturing. We show the successful adaption and realization of a silicone-based mMS dimensioned for a human model with structure sizes down to 300 µm. We elaborate the advantages and disadvantages of additive, silicone-based 3D printing for this application in comparison to molding-based and subtractive 3D printing methods, thus demonstrating the relevance of this technology for medical application.

I. Introduction

Every year, an average of 250,000 to 500,000 people worldwide suffers from a spinal cord injury (SCI) [1]. Damage to the nerve fibers in the spinal cord can restrict the transmission of impulses or cause them to fail completely. A hemi- or complete transection of the nerve fibers can consequently lead to a permanent dysfunction of the nerves and associated physical functions. In order to support the regeneration of the nerves, a concept was developed that is intended to support the re-adaptation of the nerves with the help of a combination of different therapeutic approaches [2]. The function of this mechanical microconnector system (mMS) has already been demonstrated in a rodent model by Estrada et al. [3]. Elementary features of this mMS are to bring the severed nerve fibers into close spatial proximity and optionally to deliver targeted medication to the site of injury [2]. For this purpose, it is relevant to combine a 3D structure with cavities, microchannels and honeycomb structures in the implant.

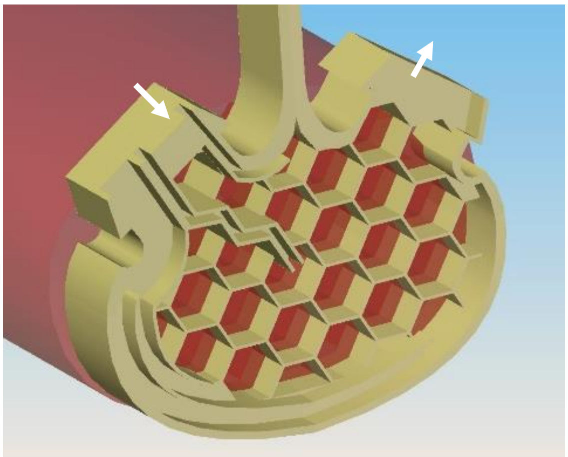

Figure 1: Functional principle of the mMS. A half-shell of the system is pictured. The nerve fibers are fixed to the honeycomb structure by temporary negative pressure and surface adhesion. Medication can be supplied through microchannels into the cavity between two half-shells. The inlet and outlet of the channels are highlighted by the arrows.

The basic structure and functional principle of such an mMS are shown in Fig. 1. SCI can occur in different positions, with different shapes and with partial or complete transection of the nerves. Acute SCI comprise primary injuries followed by secondary injuries in the following seconds to weeks due to destruction of tissue [4]. Rapid fabrication with a high degree of individualization of the structure and a biocompatible material is therefore essential for the application of the mMS in practice. The possibility of extracting a 3D printable model from medical imaging data using algorithms was demonstrated by Rengier et al [5]. Together with a fast and adaptable manufacturing method, this enables an appropriate process flow from imaging to the final mMS.

Furthermore, in addition to flexible production, the elasticity of the printed implant is also a relevant factor. Due to the natural movements of the spine, the vertebrae and associated soft tissue experience various loads and displacements [6]. A system implanted in the cross-section of the spinal cord should therefore be able to withstand these movements, making an elastic material for the mMS beneficial.

The use of an additive, three-dimensional printing process with silicone as material is suitable for the enumerated requirements. Additive 3D printing offers the possibility of flexible, rapid prototyping and silicone enables the desired elasticity of the fabricated mMS. Recent publications have demonstrated the fabrication of the mMS using bioresorbable polymer for the size of a porcine model [7,8]. In this molding-based process, cavities were realized by bonding of two fabricated half-shells. In another publication, the mMS were likewise fabricated for the size of a porcine model using selective laser-induced etching (SLE) of fused silica [9]. This subtractive fabrication approach enabled direct manufacturing of cavities within a few days. This paper deals with the fabrication of the mMS for a human model using additive 3D printing of silicone. Finally, different fabrication methods for the mMS are discussed.

II. Material and methods

In this paper, the mMS are fabricated using the Keyence AGILISTA-3200W 3D printer (Keyence Deutschland GmbH, Neu-Ilsenburg, Germany). The Agilista is a high-resolution material jetting printer, working with the deposition and subsequent UV curing of different liquid printing material and a water-soluble support material AR-S1 (Keyence Deutschland GmbH, Neu-Ilsenburg, Germany) [10]. AR-G1L (Keyence Deutschland GmbH, Neu-Isenburg, Germany), an elastic silicone material with Shore A hardness of 35, consisting of 65% silicone, 30-35% acrylate monomer, 1-5% organo phosphorus compound and 1-5% phenome compound [11], was used as printing material. Further material properties are listed in Table 1 [12].

Table 1: Material properties of the silicone printing material [12]

Mechanical properties	Unit	Value
Tensile strength	MPa	0.5-0.8
Breaking elongation	%	160
Shore A hardness	-	35
Tear resistance	kg/cm	3.1
Cured density	g/cm³	1.03
Water absorption	%	<0.4
Heat resistance	°C	150

For printing a structure, a surface model (STL) is translated into machine code using Keyence Modeling Studio software (Keyence Deutschland GmbH, Neu-Ilsenburg, Germany). After the printing, the support material has to be removed carefully in a three-step process. Firstly, most part of the model enclosing support material is manually removed. Afterwards, the model is placed in a cleansing solution (20% polyoxypropylene glycol solution, Keyence Start-up Liquid OP-87958) to remove internal support material. Lastly, the model is rinsed with deionized water.

Besides the mMS is now fabricated for human model instead of porcine model, the printing method differs from the previous mentioned fabrication methods and materials [7,8,9]. Thus, within this work, the design of mMS was adapted significantly. Critical structures of the mMS are the honeycomb geometries and further the stability of the system is crucial.

Although the elasticity of silicone as material offers advantages, it also leads to instability of the mMS. A certain stability is necessary for precise positioning of the implant during surgery and for safe guidance of the cut nerve fibers. To achieve this, the outer frame was broadened and the entire mMS was designed to be thicker. Due to the fragile honeycomb structures, especially large stresses to the material occurred at the interfaces between the honeycomb walls and the outer frame, which leads to cracks as shown in Fig. 2. This was intensified by the weight of the free-hanging honeycombs. In particular, slight manual applied torsion of the mMS leads to increased cracking. This problem was counteracted by reinforcing the transitions from the honeycomb structure to the outer frame. In addition, supporting structures between the upper and lower honeycomb levels were inserted at the intersections of the honeycombs to better distribute the load.

Moreover, the determination of an appropriate honeycomb size is a relevant issue. Ideally, the cross-sectional area covered by the walls of the honeycombs should be as small as possible and at the same time the sidewall area of the honeycombs should be as large as possible [13]. Consequently, a large number of honeycombs with a small wall thickness is desirable. Restricted by the resolution of the printing process, a too small wall thickness and likewise too large number of honeycombs is not feasible. Suitable ratios of wall thickness to number of honeycombs was determined iteratively for the intended mMS.

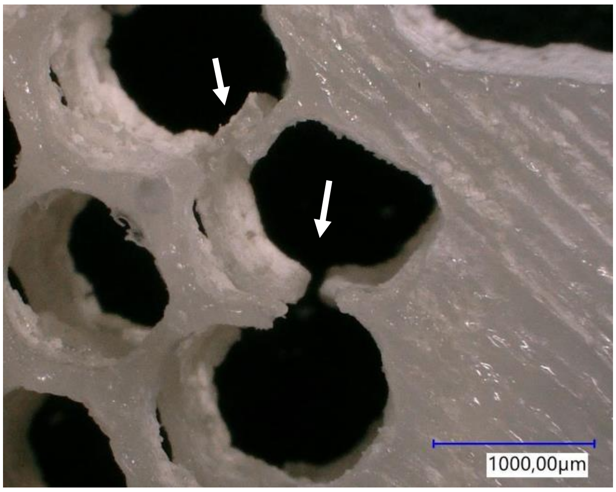

Figure 2: Cracks of the fragile honeycombs at the transition to the more stable outer sidewall of the mMS. White arrows indicate the cracks.

III. Results and discussion

Characterization of the fabricated mMS was done using a microscope. Fig. 3 shows successful fabricated mMS with different sizes of honeycombs. The top right structure exhibits significant higher ratio of covered surface by honeycomb sidewalls compared to the structures at the bottom right and left and thus there is less space left for nerve fibers to guide through the honeycombs. Therefore, the lower two structures are preferred for this application. Dimensions of this mMS are 20 mm in width and 17.5 mm in height with a total thickness of 3 mm. The honeycombs have a diameter of approximately 1.2 mm for the bottom left, respectively 1.5 mm for the bottom right structure. Sidewall thickness of the honeycombs vary at both structures between 300 µm and 370 µm. Printing time of a system is around 40 minutes.

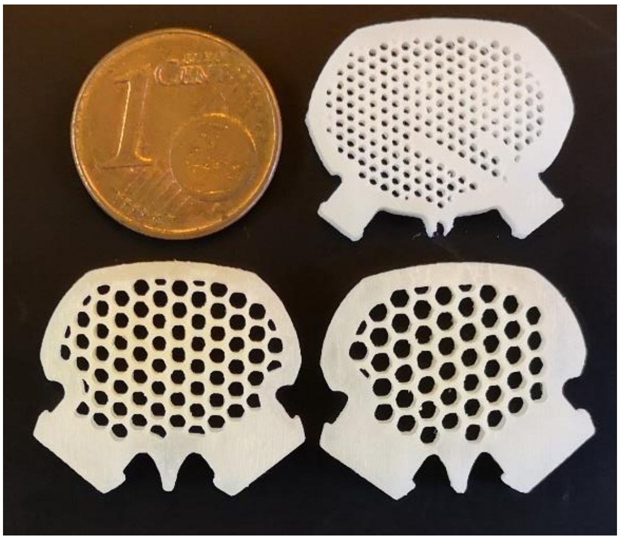

Figure 3: Top view of fabricated mMS with different honeycomb sizes in size comparison to Euro cent coin.

Further insights into the mMS are shown in Fig. 4. The angled view with visible channel input and cavity between the honeycombs is depicted in 4(A). The cross-section of a cut-through structure is given in 4(B). The support structures are visible in the center between the honeycombs. For the sidewalls of the honeycombs, a wall height of about 1.2 mm results in an aspect ratio of approximately 1:3.5. In addition, a significant surface roughness is visible on the sidewalls, which leads to a desirable better adhesion of the nerve fibers in the honeycombs. Moreover, small loads and movements were manually applied to the mMS to quantitatively test elasticity. No damage to the system was observed.

However, the production of mMS using silicone also has drawbacks compared to the previously presented methods. Table 2 compares the main properties of the methods used so far. The fabrication time for molding is significantly longer than for the other methods due to the prior preparation of a master. With the SLE process, fabrication time scales significantly with structure size due to an extended etch time. Silicone-based 3D printing therefore has an advantage in production time depending on the structure size.

Similarly, silicone as material is superior to quartz glass and polymer with regard to the elasticity of the mMS. The customisability of structures made of quartz glass and silicone is comparably high, as both materials can be structured almost arbitrarily. Furthermore, waveguides for integrated sensors can be written in structures made of quartz glass using femtosecond laser [14]. In contrast, the molding-based process is clearly restricted in design freedom due to the necessary fabrication of subsequently bonded half shells for creating cavities.

In terms of minimum achievable structure sizes, however, additive 3D printing of silicone is up to two orders of magnitude worse than the other techniques. This is an important property for the production of honeycombs. With SLE process, minimum wall thicknesses of 4µm and an aspect ratio of 1:15 could be shown for the mMS for a porcine model.

Table 2: Comparison of different printing technologies for human model mMS. '+' means above-average, 'o' average and '-' below-average compared to the other listed technologies.

Property	**Molding [7,8]**	**SLE [9]**	**Silicone 3D Printing**
Production time	-	o	+
Elasticity of material	o	-	+
Customizability	-	+	+
Minimum feature size	+	+	-

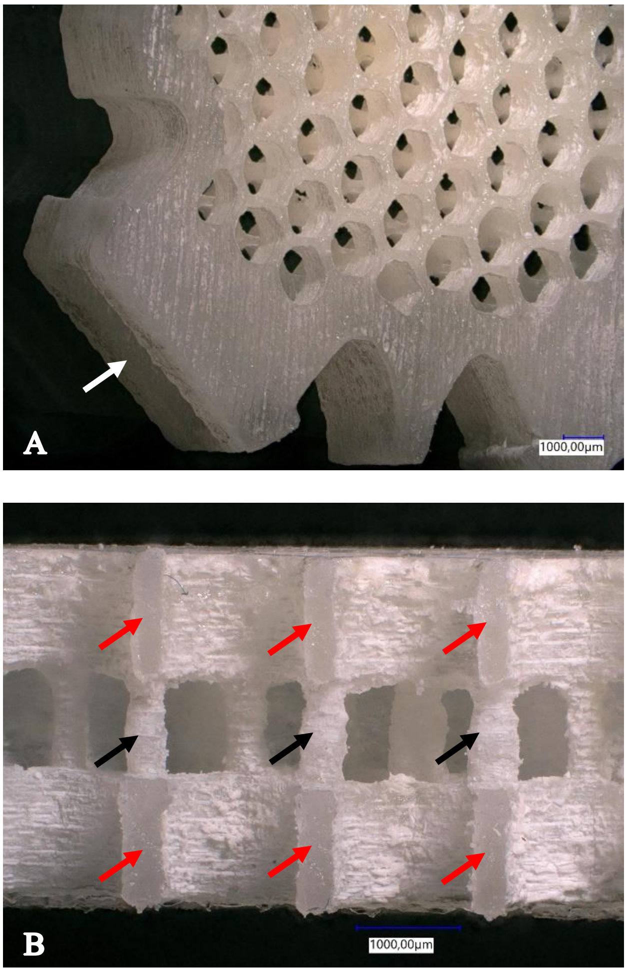

Figure 4: Insights of the fabricated mMS. (A) Tilted view under an angle of 35°. White arrow indicates the inlet of the fluidic channel. (B) Cross section of the mMS. Black arrows indicate the support structures. Red arrows indicate the cross section of the honeycomb sidewalls.

IV. Conclusions and Outlook

This work presents the successful fabrication of a silicone-based mMS for a human model using additive 3D printing. The design of the mMS was adapted to the circumstances of 3D printing silicone. A rapid prototyping with a high degree of customizability could be realized. At the same time, the necessary elasticity is possible with the required stability of the system. Due to the comparably large system in relation to the minimum structure sizes, this manufacturing method is suitable for use in human model, whereas in porcine model the previously used methods are more advantageous. In summary, this work provides a new fabrication approach for the potential application of the mMS in human model.

However, there are still some restrictions to this technique for this application, such as the very limited printing resolution and the fact that medical grade silicone is not yet available as printing material. For future research, an evaluation of the maximum possible loads and movements of the mMS at even smaller structure sizes is interesting. In addition, additive printing technologies for the mMS can be investigated with alternative materials.

Acknowledgments

The Authors would like to thank BMBF for the funding of ForLab HELIOS (funding reference number 16ES0945K) which provides the 3D printer for this investigation.

Author's statement

Authors state no conflict of interest. Informed consent has been obtained from all individuals included in this study.

References

[1] World Health Organization, and International Spinal Cord Society. International perspectives on spinal cord injury. World Health Organization, 2013.

[2] Seide, Klaus, et al. "Rückenmarkadaptation." Trauma und Berufskrankheit 15.2 (2013): 179-184.

[3] Estrada, Veronica, et al. "Low-pressure micro-mechanical re-adaptation device sustainably and effectively improves locomotor recovery from complete spinal cord injury." Communications biology 1.1 (2018): 1-11.

[4] Witiw, Christopher D., et al. "Acute spinal cord injury." Journal of Spinal Disorders and Techniques 28.6 (2015): 202-210.

[5] Rengier, Fabian, et al. "3D printing based on imaging data: review of medical applications." International journal of computer assisted radiology and surgery 5.4 (2010): 335-341.

[6] Friis, E. A., et al. "Mechanical testing of cervical, thoracolumbar, and lumbar spine implants." Mechanical Testing of Orthopaedic Implants. Woodhead Publishing, 2017. 161-180.

[7] von Poblotzki, Jana M., et al. "Advances in manufacturing of biodegradable spinal cord implants on microscale through micromolding and 3D printing." 2019 20th International Conference on Solid-State Sensors, Actuators and Microsystems & Eurosensors XXXIII (TRANSDUCERS & EUROSENSORS XXXIII). IEEE, 2019.

[8] von Poblotzki, Jana Marina, et al. "Integration of subtractive 3D printing into micromolding of biodegradable implants for spinal cord treatment." Transactions on Additive Manufacturing Meets Medicine 1.1 (2019).

[9] Rennpferdt, Lukas, et al. "Advances in manufacturing spinal cord implant using 3D selective laser induced etching of fused silica." Transactions on Additive Manufacturing Meets Medicine 3.1 (2021): 574-574.

[10] Keyence Deutschland GmbH, "Modellreihe AGILISTA 3D-Drucker Katalog", 2020.

[11] Keyence Deutschland GmbH, „AR-G1L Sicherheitsdatenblatt", 2017

[12] Keyence Deutschland GmbH, „Materialdatenblatt Modellreihe AGILISTA Serie-3000",2016.

[13] Voss, Christian, et al. Mikrosystem Zur Funktionellen Regeneration Des Rückenmarks Bei Hemi- Und Totaltranssektion. 1. Aufl. München: Dr. Hut, 2012.

[14] Tan, Dezhi, et al. "Femtosecond laser writing low-loss waveguides in silica glass: highly symmetrical mode field and mechanism of refractive index change." Optical Materials Express 11.3 (2021): 848-857.